

## Supporting Information

### **Cold Field Electron Emission of Large-area Arrays of SiC Nanowires: Spatial Analysis, Photo-Enhancement and Saturation Effects.**

*Stefania Carapezzi,<sup>\* a◇</sup> Antonio Castaldini,<sup>a</sup> Filippo Fabbri,<sup>b‡</sup> Francesca Rossi,<sup>b</sup> Marco Negri,<sup>b§</sup>  
Giancarlo Salviati,<sup>b</sup> and Anna Cavallini<sup>a</sup>*

<sup>a</sup> Department of Physics and Astronomy, University of Bologna, Viale Berti Pichat 6/2, 40127,  
Bologna, Italy

<sup>b</sup> IMEM-CNR Parco Area delle Scienze 37/A, 43124, Parma, Italy

◇ University of Bologna (ARCES - DEI), Viale Risorgimento 2, 40136 Bologna, Italy

‡ KET Lab c/c Italian Space Agency via del Politecnico, 00133, Roma, Italy

§ Laboratoire des Matériaux Semiconducteurs, École Polytechnique Fédérale de Lausanne,  
Lausanne, Switzerland

\* Address correspondence to stefania.carapezzi@gmail.com

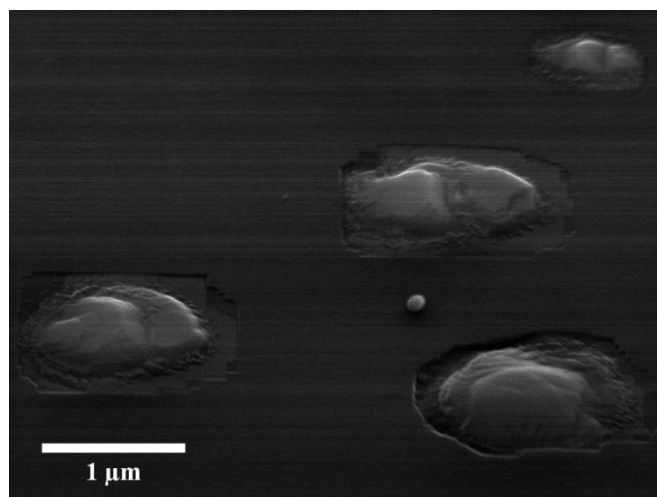


**Fig. S1** Nickel mounds after melting and dewetting of the surface, before SiC NWs growth.

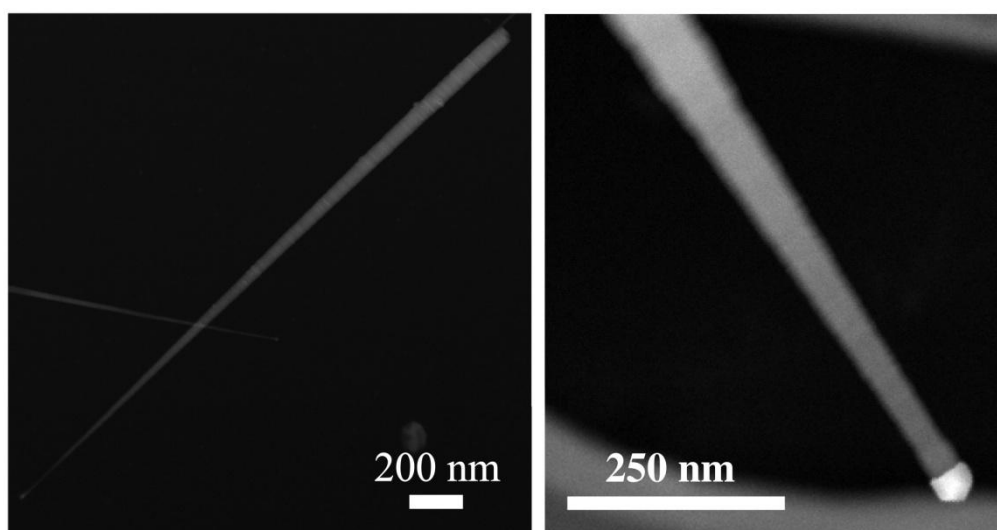


**Fig. S2** STEM-HAADF overview of single SiC NWs. The presence of the catalyst on the tip of the nanowires is an evidence of the VLS float growth<sup>S1</sup> and a confirmation comes from the tapered shape of the wires: the cause of that can be the radial growth at the base or the catalyst consumption during the growth<sup>S2</sup>.

## Fowler-Nordheim Theory for Metals

According to standard FN theory,<sup>1</sup> the FE current density for a flat, clean metal surface is described by

$$J = \frac{A}{\varphi} E_0^2 \exp\left(-\frac{B\varphi^{\frac{3}{2}}}{E_0}\right) \quad (\text{S1})$$

set that  $E_0 = V/d$  is the applied field,  $V$  is the applied voltage,  $d$  is the inter-electrodes gap,  $\varphi$  is the work function of the electron-emitting material,  $A = 1.54 \cdot 10^{-6} \text{ eV/V}^2$  and  $B = 6.83 \cdot 10^3 \text{ V} \cdot \text{eV}^{3/2}/\mu\text{m}$  are constants. Equation (S1) is a 1-dimensional approximation which gives a correct description of experimental FE current densities from 0 K up to room temperature. Equation (1) holds for ideally smooth metal surfaces, but it still describes correctly CFE currents from real emitters decorated by a superficial micro-roughness provided that the electric field is now expressed by  $E = \beta V/d = \beta E_0$ ,  $\beta$  being the so-called “field enhancement factor”. Equation (S1) can then be rearranged in the following way

$$\ln\left(\frac{I}{E_0^2}\right) = \ln\left(\frac{A}{\varphi} \cdot \beta^2 \cdot area\right) - \frac{B\varphi^{\frac{3}{2}}}{\beta} \cdot \frac{1}{E_0} \quad (\text{S2})$$

where *area* is the effective emitting area. In fact, experimental data show that FE currents do not originate from the whole surface of metallic macro-cathodes, but they are restricted to the micron-sized protrusions constituting the surface roughness.

## CFE from LAFE systems

The emission current from LAFE systems comes, actually, only from a limited fraction of the total substrate area. To take this into account it has been introduced<sup>64</sup> the parameter “area efficiency of emission”  $\alpha$ , defined as the ratio between the so-called “notional emission area”  $A_n$  and the “macroscopic area” or total area of the substrate  $A_M$ .  $A_n$  is defined according to<sup>64</sup>

$$I = \int_{A_M} J_L dA = J_0 A_n \quad (\text{S3})$$

provided that  $I$  is the total current from an emitter of macroscopic area  $A_M$ ,  $J_L$  is the local CFE current density dependent on position over the emitter surface, and  $J_0$  is the maximum local CFE current density, where the label  $0$  refers to the position on the emitting surface at which  $J_L$  is highest at the given applied voltage.

**Table S1** Review of CFE of SiC nanostructures under dark conditions.

CFE from SiC nanostructures under dark conditions			
1D field emitters	Threshold field, $E_{Th}$ [V / $\mu\text{m}$ ]	Turn-on field, $E_{TO}$ [V / $\mu\text{m}$ ]	References
SiC NWs on a silicon synthesized by hot-filament-assisted CVD with a solid silicon and carbon source.	30 at a current density of 10 mA/cm <sup>2</sup>	20	Wong et al. <sup>33</sup>
FE measurements at pressure of about $5 \cdot 10^{-8}$ Torr			
Bunches of SiC NWs grown by SiC and Fe powders through heating.	8.5	5	Wu et al. <sup>34</sup>
FE measurements at pressure of about $10^{-10}$ Torr.			
Core-shell SiC-SiO <sub>2</sub> NWs synthesized by direct heating the NiO-coated silicon substrate under reductive environment by the carbothermal reduction of WO <sub>3</sub> by C; thickness of SiO <sub>2</sub> was varied through HF-etching.	-	4.0 (bare SiC NWs), 3.3 (10 nm SiO <sub>2</sub> -coated SiC NWs) and 4.5 (20 nm SiO <sub>2</sub> -coated SiC NWs).	Ryu et al. <sup>35</sup>
FE measurements at pressure of about $1 \cdot 10^{-4}$ Torr.			
SiC NWs grown from the surface of SiC bulk ceramic substrate by catalyst-assisted thermal heating.	5.77	3.33	Deng et al. <sup>36</sup>
FE measurements at pressure of about $10^{-8}$ Torr.			
$\beta$ -SiC NWS obtained by thermal evaporation of SiO powders onto activated C fibers.	-	3.1 – 3.5	Zhou et al. <sup>37</sup>
FE measurements at pressure of $3 \cdot 10^{-5}$ Pa.			
Ga-catalyzed VLS-grown bamboo-like $\beta$ -SiC NWs; highly faceted hexagonal cross-sections and sharp corners.	-	10	Shen et al. <sup>38</sup>
FE measurements at pressure of about $5 \cdot 10^{-7}$ Torr.			
Hierarchical single-crystalline $\beta$ -SiC nanoarchitectures.	-	12	Shen et al. <sup>39</sup>
FE measurements at pressure of about $1.1 \cdot 10^{-5}$ Torr; report of two linear regimes.			

CFE from SiC nanostructures under dark conditions			
1D field emitters	Threshold field, $E_{Th}$ [V / $\mu\text{m}$ ]	Turn-on field, $E_{To}$ [V / $\mu\text{m}$ ]	References
VS-grown SiC nanowires arrays on Si substrate.	10.5 (aligned NWs); 29.5 (random oriented NWs)	14 (aligned NWs); 37 (random oriented NWs)	Niu et al. <sup>40</sup>
FE measurements at pressure of about $5 \cdot 10^{-5}$ Pa.			
MOCVD-grown $\beta$ -SiC NWs.	2 (for $I_{Th} = 5$ nA, corresponding to a current density of $0.025 \mu\text{A}/\text{cm}^2$ ;	-	Kim et al. <sup>41</sup>
FE measurements at pressure of about $10^{-7}$ Torr; $\beta(\varphi(\text{SiC}) = 5 \text{ eV}) = 2000$ .			
Microwave assisted vapor-solid-grown ultrathin 3C-SiC nanobelts.	-	3.2	Wei et al. <sup>42</sup>
FE measurements at pressure of about $4 \cdot 10^{-7}$ Pa.			
Porous SiC NWs obtained through carbonizing of metal-assisted chemically etched silicon NWs.	-	Dependent on the anode-cathode distance $d$ : 2.9, 2.6 and 2.3 for $d = 300, 400$ and $500 \mu\text{m}$	Yang et al. <sup>43</sup>
FE measurements at pressure of about $2 \cdot 10^{-4}$ Pa; $\beta(\varphi(\text{SiC}) = 4.53 \text{ eV}) = 5241$ .			
Catalyst-free tubular $\beta$ -SiC nanostructures.	10 at a current density of $10 \text{ mA}/\text{cm}^2$	$< 5$	Cui et al. <sup>44</sup>
The pressure at which FE were performed was not reported.			
$\beta$ -SiC NWs Felted NWs (catalyst-free on graphite substrate), curly NWs (catalyst-free on Si substrate), straight NWs (Ni-catalyzed on graphite substrate).	5.3 (felted NWs) / 3.25 (curly NWs) / 2 (straight NWs)	2 (felted NWs) / 1.5 (curly NWs) / 1 (straight NWs); at a current density of $10 \text{ mA}/\text{cm}^2$	Li et al. <sup>45</sup>
FE measurements at pressure of about $10^{-8}$ Torr.			
Al-doped 3C-SiC (bunch-like) NWs.	1.38 - 1.54	0.55 – 0.85	Zhang et al. <sup>S3</sup>
FE measurements at pressure of about $7 \cdot 10^{-5}$ Pa; $\varphi(\text{SiC}) = 5 \text{ eV}$ .			

CFE from SiC nanostructures under dark conditions			
1D field emitters	Threshold field, $E_{Th}$ [V / $\mu\text{m}$ ]	Turn-on field, $E_{TO}$ [V / $\mu\text{m}$ ]	References
Al <sub>2</sub> O <sub>3</sub> decorated and bare tubular $\beta$ -SiC (bunch-like) nanostructures.	23.5 (bare $\beta$ -SiC nanostructures) / 5.37 (Al <sub>2</sub> O <sub>3</sub> decorated $\beta$ -SiC nanostructures) at a current density of 10 mA/cm <sup>2</sup>	8.8 (bare $\beta$ -SiC nanostructures) / 2.4 (Al <sub>2</sub> O <sub>3</sub> decorated $\beta$ -SiC nanostructures)	Cui et al. <sup>46</sup>
The pressure at which FE were performed was not reported.			
Lawn-like 3C-SiC NWs; hexagonal cross section; presence of microtwins and SFs.	-	2.1	Chen et al. <sup>47</sup>
FE measurements at pressure of about $5 \cdot 10^{-5}$ Torr; report of two linear regimes			
3C-SiC nanoneedles synthesized by catalyst-assisted pyrolysis of polyaluminasilazane precursors; concentration of Al = 0.7 %.	-	1.3 (RT)	Wei et al. <sup>54</sup>
FE measurements at pressure of about $5 \cdot 10^{-7}$ Pa; range of temperature: RT – 500 °C.			
Two-step VS-grown $\beta$ -SiC nanobelts with a median ridge (NW with two lateral flakes); presence of SFs.	-	3.2	Meng et al. <sup>55</sup>
FE measurements at pressure of about $10^{-7}$ Torr.			
CVD-grown nonaligned-SiC NWs on Si nanoporous pillar array; presence of SFs.	-	2.9	Wang et al. <sup>56</sup>
FE measurements at pressure of about $2 \cdot 10^{-7}$ Pa; $\phi(\text{SiC}) = 4.4$ eV.			
1,10-phenanthroline-assisted molecule template $\beta$ -SiC NWs; presence of SFs.	8.12	3.57	Xi et al. <sup>57</sup>
The pressure at which FE were performed was not reported.			
Fe-assisted VLS-grown $\beta$ -SiC NWs on flexible carbon fabric; hexagonal cross section; presence of microtwins and SFs.	-	1.2	Wu et al. <sup>58</sup>
FE measurements at pressure of about $5 \cdot 10^{-5}$ Pa; $\beta(\phi(\text{SiC}) = 4.0 \text{ eV}) = 3368$ .			

CFE from SiC nanostructures under dark conditions			
1D field emitters	Threshold field, $E_{Th}$ [V / $\mu\text{m}$ ]	Turn-on field, $E_{To}$ [V / $\mu\text{m}$ ]	References
N-doped quasialigned 3C-SiC NWs via the pyrolysis of polymeric precursor with $\text{Co}(\text{NO}_3)_2$ as the catalyst; concentration of N = 2.38 %; presence of SFs.	2.53–3.51;	1.90–2.65	Chen et al. <sup>S9</sup>
FE measurements at pressure of about $3 \cdot 10^{-7}$ Pa; $\beta(\varphi(\text{SiC}) = 4.0 \text{ eV}) = 1710$ .			
CVD-grown 3C-SiC nanoneedles synthesized on carbon cloth; presence of SFs.	2.2	1.3	Wu et al. <sup>S10</sup>
FE measurements at pressure of about $5 \cdot 10^{-5}$ Pa; $\beta(\varphi(\text{SiC}) = 4.0 \text{ eV}) = 3667$ .			
3C-SiC nanoneedles on highly flexible carbon fabric via the catalyst assisted pyrolysis of polysilazane; presence of SFs and twins.	2.2 (undoped nanoneedles); 1.7 – 2 (N-doped nanoneedles; concentration of N = 3 %)	1.6 (undoped nanoneedles); 1.1 - 1.35 (N-doped nanoneedles; concentration of N = 3 %)	Zhang et al. <sup>S11</sup>
CVD-grown 3C-SiC nanoneedles synthesized on carbon cloth; presence of SFs.			
Quasialigned SiC nanoarrays with sharp tips via catalyst assisted pyrolysis of polymeric precursors on carbon fabric; concentration of N = 3.35 %; presence of SFs.	-	2.19 – 1.15	Chen et al. <sup>S12</sup>
FE measurements at pressure of about $1.5 \cdot 10^{-7}$ Pa.			
$\text{H}_2$ and $\text{N}_2$ plasma-treated $\beta$ -SiC NWs.	6.7 (10 minutes of $\text{H}_2$ -treatment); 6.3 (20 minutes of $\text{H}_2$ -treatment); 6.0 (10 minutes of $\text{N}_2$ -treatment); at a current density of $10 \text{ mA/cm}^2$	3.2 (10 minutes of $\text{H}_2$ -treatment); 3.0 (20 minutes of $\text{H}_2$ -treatment); 2.8 (10 minutes of $\text{N}_2$ -treatment)	Li et al. <sup>S13</sup>
FE measurements at pressure of about $10^{-7}$ Torr.			



CFE from SiC nanostructures under dark conditions

1D field emitters	Threshold field, $E_{Th}$ [V / $\mu\text{m}$ ]	Turn-on field, $E_{To}$ [V / $\mu\text{m}$ ]	References
B-doped 3C-SiC nanowires via catalyst assisted pyrolysis of polymeric precursor; triangular prism-like body. B-doped NWs: concentration of B = 5.03 %, density of $1.3 \cdot 10^{-6}$ NW/cm <sup>2</sup> , very rough sidewalls and presence of SFs; undoped NWs: $2.3 \cdot 10^{-6}$ NW/cm <sup>2</sup> and smoother sidewalls.	1.7 (B-doped nanoneedles)	1.35 (B-doped nanoneedles)	Yang et al. <sup>S14</sup>
FE measurements at pressure of about $3 \cdot 10^{-7}$ Pa; $\beta(\phi(\text{SiC}) = 4.0 \text{ eV}) = 4895$ .			
N-doped SiC nanoneedles via catalyst-assisted pyrolysis of polysilazane precursor, on carbon fabrics.	1.79 (concentration of N = 4.39 %), 1.64 (concentration of N = 6.01 %), 1.55 (concentration of N = 7.58 %)	1.38 (concentration of N = 4.39 %), 1.22 (concentration of N = 6.01 %), 1.11 (concentration of N = 7.58 %)	Chen et al. <sup>S15</sup>
FE measurements at pressure of about $1.5 \cdot 10^{-7}$ Pa; $\phi(\text{SiC}) = 4.0 \text{ eV}$ .			
n-type SiC NWs via Au-assisted pyrolysis of polyureasilazane on 6H-SiC wafer substrates; concentration of N = 3.01 %; density of $5.7 \cdot 10^7$ NWs / cm <sup>2</sup> .	2.65 (RT); 1.33 (500°C)	1.50 (RT); 0.94 (500°C)	Wang et al. <sup>S16</sup>
FE measurements at pressure of about $1.5 \cdot 10^{-7}$ Pa; range of temperature: RT – 500 °C; $\beta(\phi(\text{SiC}) = 4.0 \text{ eV}; \text{RT}) = 4482$ .			
n-type SiC NWs via Au-assisted pyrolysis of polyureasilazane on 6H-SiC wafer substrates; concentration of N = 3.01 %; density of $5.7 \cdot 10^7$ NWs / cm <sup>2</sup> .	2.69 ( $2.9 \cdot 10^7$ NWs / cm <sup>2</sup> ); 2.34 ( $4.0 \cdot 10^7$ NWs / cm <sup>2</sup> ); 2.96 ( $5.7 \cdot 10^7$ NWs / cm <sup>2</sup> );	1.79 ( $2.9 \cdot 10^7$ NWs / cm <sup>2</sup> ); 1.57 ( $4.0 \cdot 10^7$ NWs / cm <sup>2</sup> ); 1.95 ( $5.7 \cdot 10^7$ NWs / cm <sup>2</sup> )	Wang et al. <sup>S17</sup>
FE measurements at pressure of about $1.5 \cdot 10^{-7}$ Pa; $\phi(\text{SiC}) = 4.0 \text{ eV}$ ; $\beta(2.9 \cdot 10^7 \text{ NWs / cm}^2) = 3300$ , $\beta(4.0 \cdot 10^7 \text{ NWs / cm}^2) = 3340$ , $\beta(5.7 \cdot 10^7 \text{ NWs / cm}^2) = 3217$ .			
B-doped SiC NWs via the catalyst-assisted pyrolysis of polyborosilazanes on 6H-SiC wafer substrates; concentration of B = 5.3 %; density of $3.9 \cdot 10^7$ NWs / cm <sup>2</sup> .	3.21 (RT); 1.33 (500°C)	1.92 (RT); 0.98 (500 °C)	Wang et al. <sup>S18</sup>
FE measurements at pressure of about $2.0 \cdot 10^{-7}$ Pa; range of temperature: RT – 500 °C; $\beta(\phi(\text{SiC}) = 4.0 \text{ eV}) = 3643$ .			
N-doped SiC nanoneedles via catalyst-assisted pyrolysis of polysilazane precursor, on carbon fabrics; concentration of N = 2.75 %.	-	1.58 (RT); 0.65 (500 °C)	Ying et al. <sup>S19</sup>
FE measurements at pressure of about $3.0 \cdot 10^{-7}$ Pa; range of temperature: RT – 500 °C; $\beta(\phi(\text{SiC}) = 4.0 \text{ eV}) = 2671$ .			

CFE from SiC nanostructures under dark conditions			
1D field emitters	Threshold field, $E_{Th}$ [V / $\mu\text{m}$ ]	Turn-on field, $E_{To}$ [V / $\mu\text{m}$ ]	References
Undoped and N-doped SiC nanoneedles.	6.9 (undoped nanoneedles), 5.6 (concentration of N = 0.975 %), 4 (concentration of N = 1.336 %), 6.3 (concentration of N = 2.265 %)	2.9 (undoped nanoneedles), 1.9 (concentration of N = 0.975 %), 1.5 (concentration of N = 1.336 %), 2.1 (concentration of N = 2.265 %)	Zhao et al. <sup>S20</sup>
FE measurements at pressure of about $10^{-8}$ Torr.			
Bare and Au-decorated SiC NWs grown via pyrolysis of polysilazane precursor, on carbon fabrics.	2.75 (bare NWs), 1.75 (Au-decorated NWs)	2.1 (bare NWs), 1 (Au-decorated NWs)	Chen et al. <sup>S21</sup>
FE measurements at pressure of about $1.5 \cdot 10^{-7}$ Pa; $\phi(\text{SiC}) = 4.0$ eV; $\beta(\text{bare NWs}) = 1150$ , $\beta(\text{Au-decorated NWs}) = 6244$ .			
Gourd-shaped N-doped 4H-SiC NWs via an electrochemical anodic oxidation process; concentration of N = 2.75 %.	-	0.95 (RT)	Chen et al. <sup>S22</sup>
FE measurements at pressure of about $1.5 \cdot 10^{-7}$ Pa; range of temperature: RT – 200 °C; $\beta(\phi(\text{SiC}) = 4.0 \text{ eV}) = 4370$ .			

**Table S2** Review of CFE of semiconductor NWs under photon excitation

CFE under light conditions				
1D field emitters	Notes	Threshold field, $E_{Th}$ [V / $\mu\text{m}$ ]	Turn-on field, $E_{To}$ [V / $\mu\text{m}$ ]	References
CuO nanobelts	Pressure of $5 \cdot 10^{-7}$ Pa; halogen lamp	-	-	Chen et al. <sup>S23</sup>
ZnO NWs	Pressure of $5 \cdot 10^{-6}$ Torr; UV lamp at 362 nm	-	5.1(dark) / 2.1 (light) at a current density of $1 \mu\text{A}/\text{cm}^2$	Chen et al. <sup>55</sup>
CuO NWs	Pressure of $4 \cdot 10^{-6}$ Torr; UV lamp at 365 nm	-	8.3 (dark) / 7.5 (light) at a current density of $10 \mu\text{A}/\text{cm}^2$	Juan et al. <sup>53</sup>
TiO <sub>2</sub> nanostructures	Pressure of about $10^{-5}$ Pa; UV lamp at 365 and 405 nm	-	-	Wakaya et al. <sup>S24</sup>
$\beta$ -Ga <sub>2</sub> O <sub>3</sub> NWs	Pressure of $5 \cdot 10^{-6}$ Torr; UV lamp emitting at 254 nm	-	2 (dark) / 1.2 (light) at a current density of $10 \mu\text{A}/\text{cm}^2$	Wu et al. <sup>54</sup>
undoped and In-doped ZnO nanorods	Pressure $< 5 \cdot 10^{-6}$ Torr; He-Cd laser (325 nm)	-	5.4 (undoped; dark), 0.8 (doped; dark) / 3.8 (undoped, light), 0.24 (doped, light)	Chang et al. <sup>56</sup>
Ga-doped ZnO nanorods	Pressure $< 5 \cdot 10^{-6}$ Torr; He-Cd laser (325 nm)	-	3.63 (dark), 3.15 (light)	Hsiao et al. <sup>S25</sup>
Undoped and Ga-doped ZnO nanorods	Pressure $< 5 \cdot 10^{-6}$ Torr; UV 325-nm light	-	5.4 (undoped, dark), 3.6 (doped, dark) / 3.8 (undoped, light), 3.1 (doped, light)	Chang et al. <sup>57</sup>
Mg-doped ZnO nanorods	Pressure $< 5 \cdot 10^{-6}$ Torr; UV 365-nm light	-	2.27 (dark) / 1.97 (light)	Liu et al. <sup>58</sup>
Bare and Ag-decorated ZnO nanorods	Pressure $< 5 \cdot 10^{-6}$ Torr; UV 365-nm light	-	6.7 (bare, dark), 3.93 (Ag-decorated, dark) / 3.87 (bare, light), 2.04 (doped, light)	Yang et al. <sup>59</sup>

## Additional References for Supporting Information

- S1 K. W. Kolasinski, *Curr. Opin. Solid State Mater. Sci.*, 2006, **10**, 182.
- S2 K. W. Schwarz and J. Tersoff, *Phys. Rev. Lett.*, 2009, **102**, 206101.
- S3 X. Zhang, Y. Chen, Z. Xie and W. Yang, *J. Phys. Chem. C*, 2010, **114**, 8251.
- S4 G. Wei, H. Liu, C. Shi, F. Gao, J. Zheng, G. Wei and W. Yang, *J. Phys. Chem. C*, 2011, **115**, 13063.
- S5 A. Meng, M. Zhang, J. Zhang, and Z. Li, *Cryst. Eng. Comm.*, 2012, **14**, 6755.
- S6 H. Wang, and Z. Li, L. Kang, and X. Li, *Appl. Surf. Sci.*, 2012, **259**, 79.
- S7 G. Xi, Y. He, and C. Wang, *Chemistry – A European Journal*, 2010, **16**, 5184.
- S8 R. Wu, K. Zhou, J. Wei, Y. Huang, F. Su, J. Chen and L. Wang, *J. Phys. Chem. C*, 2012, **116**, 12940.
- S9 S. Chen, P. Ying, L. Wang, G. Wei, J. Zheng, F. Gao, S. Su and W. Yang, *J. Mater. Chem. C*, 2013, **1**, 4779.
- S10 R. Wu, K. Zhou, X. Qian, J. Wei, Y. Tao, C. H. Sow, L. Wang, Y. Huang, *Materials Letters*, 2013, **91**, 220.
- S11 X. Zhang, Y. Chen, W. Liu, W. Xue, J. Li and Z. Xie, *J. Mater. Chem. C*, 2013, **1**, 6479.
- S12 S. Chen, P. Ying, L. Wang, F. Gao, G. Wei, J. Zheng, Z. Xie, and W. Yang, *RSC Adv.*, 2014, **4**, 8376.
- S13 Z. Li, W. Li, X. Wang, and M. Zhang, *Phys. Status Solidi A*, 2014, **211**, 1550.
- S14 Y. Yang, H. Yang, G. Wei, L. Wang, M. Shang, Z. Yang, B. Tang and W. Yang, *J. Mater. Chem. C*, 2014, **2**, 4515.
- S15 S. Chen, P. Ying, L. Wang, G. Wei, W. Yang, *Appl. Phys. Lett.*, 2014, **105**, 133106.
- S16 L. Wang, C. Li, Y. Yang, S. Chen, F. Gao, G. Wei, W. Yang, *ACS Applied Materials and Interfaces*, 2015, **7**, 526.
- S17 L. Wang, F. Gao, S. Chen, C. Li and W. Yang, *Appl. Phys. Lett.*, 2015, **107**, 122108.
- S18 L. Wang, G. Wei, F. Gao, C. Li and W. Yang, *Nanoscale*, 2015, **7**, 7585.
- S19 P.-Z. Ying, S.-L. Chen, X.-L. Ren, and Q. Chen, *Superlattices and Microstructures*, 2015, **86**, 250.
- S20 J. Zhao, A. Meng, M. Zhang, W. Ren, and Z. Li, *Phys. Chem. Chem. Phys.*, 2015, **17**, 28658.
- S21 Q. Chen, S. Chen, F. Gao, L. Wang, Z. Xie, and W. Yang, *J. Mater. Chem. C*, 2016, **4**, 1363.
- S22 C. Chen, S. Chen, M. Shang, F. Gao, Z. Yang, Q. Liu, Z. He, W. Yang, *J. Mater. Chem. C*, 2016.
- S23 J. Chen, N. Y. Huang, S. Z. Deng, J. C. She, N. S. Xu, W. Zhang, X. Wen, S. Yang, *Appl. Phys. Lett.*, 2005, **86**, 151107.
- S24 F. Wakaya, T. Tatsumi, K. Murakami, S. Abo, M. Takai, T. Takimoto, Y. Takaoka, *J. Vac. Sci. Technol., B: Nanotechnol. Microelectron.: Mater., Process., Meas., Phenom.*, 2011, **29**, 02B110.
- S25 C. H. Hsiao, C. S. Huang, S. J. Young, S. J. Chang, J. J. Guo, C. W. Liu, and T. Y. Yang, *IEEE Trans. on Electron Devices*, 2013, **60**, 1905.